**Rapid biosensor of SARS-CoV-2 using specific monoclonal antibodies recognizing conserved nucleocapsid protein epitopes**

Jong-Hwan Lee[a], Yujin Jung[a], Sung-Kyun Lee[a], Jung Kim[a], Chang-Seop Lee[b], Soohyun Kim[a], Ji-Seon Lee[a], Nam-Hoon Kim[a, *], and Hong-Gi Kim[a,*]

[a] *Center for Convergent Research of Emerging Virus Infection, Korea Research Institute of Chemical Technology, Daejeon 34114, Republic of Korea*

[b]*Department of Internal Medicine, Jeonbuk National University Medical School, Jeonju, Jeollabuk-do 54896, Republic of Korea; Biomedical Research Institute of Jeonbuk National University Hospital, Jeonju, Jeollabuk-do 54907, Republic of Korea*

* Co-Corresponding authors: nhkim@krict.re.kr and Hong Gi Kim (tenork@krict.re.kr)

## Supplementary Information

## Supplementary Figures

**Figure S1.** Sequence alignment of SARS-CoV-2 NP antigen with SARS-CoV NP, MERS-CoV NP, 229E, and OC43.

**Figure S2.** Schematic illustration of the SARS-CoV-2 viral components.

**Figure S3.** Bar graph showing secondary screening results using indirect LFIA.

**Figure S4.** Biolayer interferometry (BLI) results of monoclonal antibodies against antigenic peptides.

**Figure S5.** Brightness and saturation adjusted images of the LFIA results for each of selected six pairs.

**Figure S6.** Optimization of detection probe by adjusting the mixing ratio of 54G6 and 54G10.

**Figure S7.** Brightness and saturation adjusted images of the LFIA results in the low concentration range for the sensitivity analysis.

**Figure S8.** Brightness and saturation adjusted images of the LFIA results Detection sensitivity results of pair 1-based LFIA with clinical specimens.

**Figure S9.** Detection sensitivity of the Pair 2-based LFIA with clinical specimens (n = 16).

**Figure S10.** Pair 1- and Pair 2-based LFIA results using negative samples from healthy donors (n = 10).

**Figure S11.** Results of RT-qPCR analysis with nasopharyngeal swabs from COVID-19 patients (n = 16) and healthy donors (n = 10).

**Figure S12.** Analysis of the specificity of Pair 1- and Pair 2-based LFIA.

## Supplementary Tables

**Table S1.** Detailed information for COVID-19 patients (n = 16) and healthy donors (n = 10).

## Figure S1

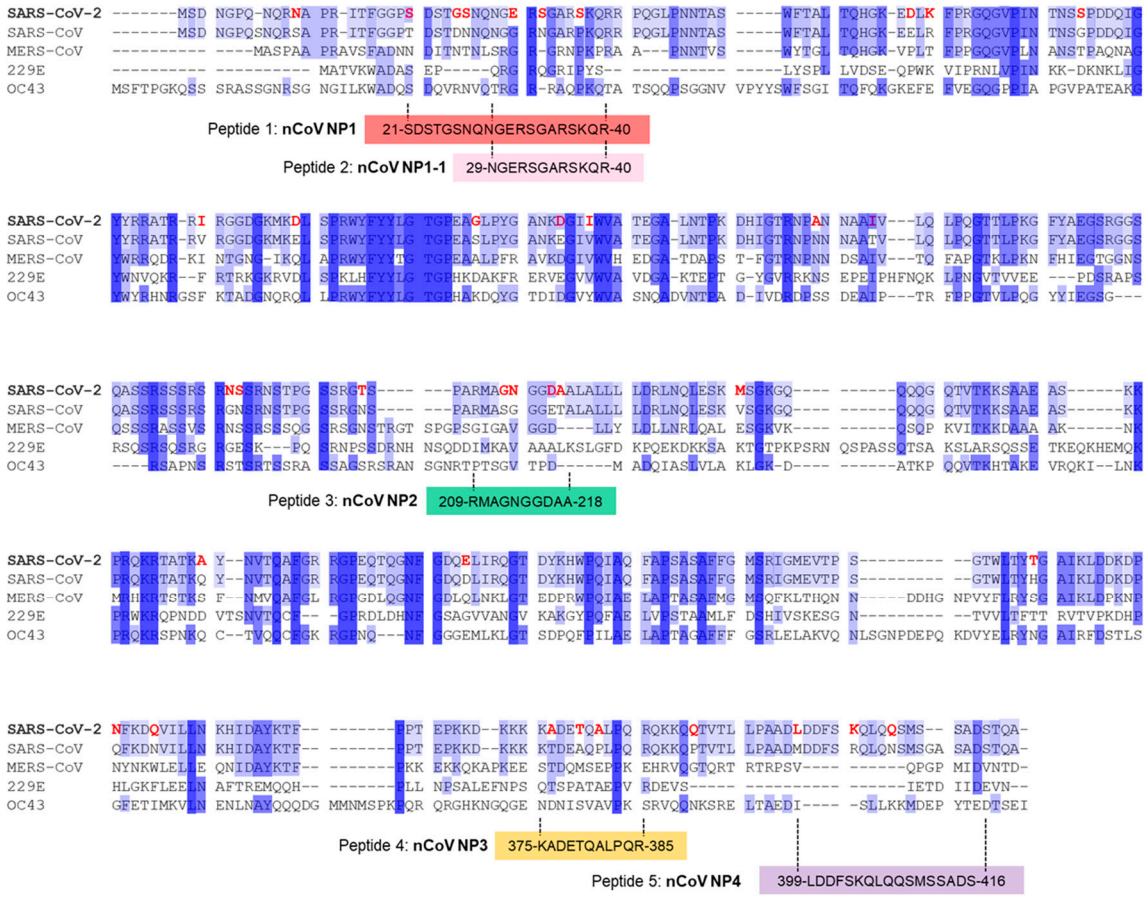



**Figure S1. Sequence alignment of SARS-CoV-2 NP antigen with SARS-CoV NP, MERS-CoV NP, 229E, and OC43.** SARS-CoV2 NP shares high sequence homology with NPs from SARS-CoV (~90% identity) and MERS-CoV (~50% identity). Five SARS-CoV-2-specific peptides with sequence specificity were selected as antigenic determinants.

**Figure S2**

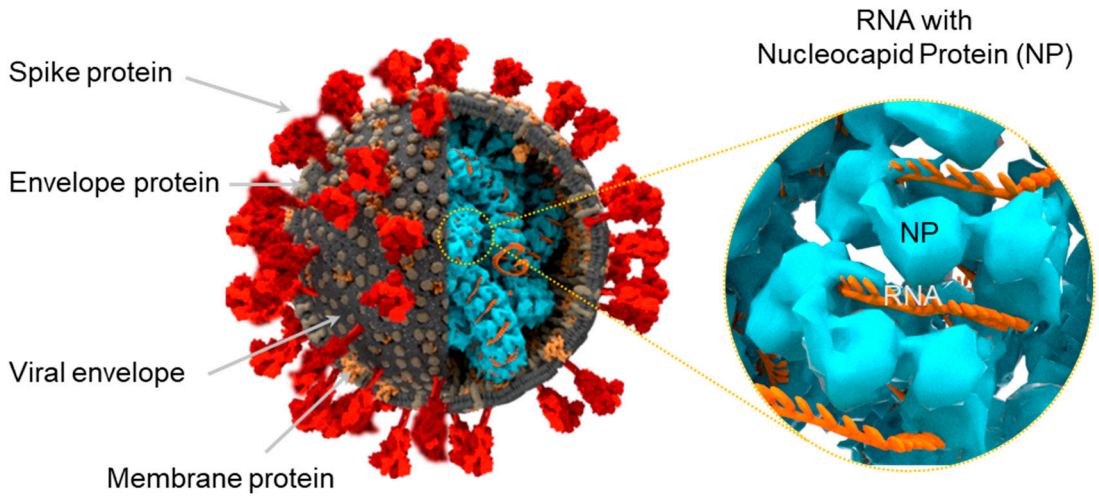



**Figure S2. Schematic illustration of the SARS-CoV-2 viral components.** NP (cyan) binds to single-stranded RNA (orange) in a helical capsid structure and plays a crucial role in packaging the viral genome.

**Figure S3**

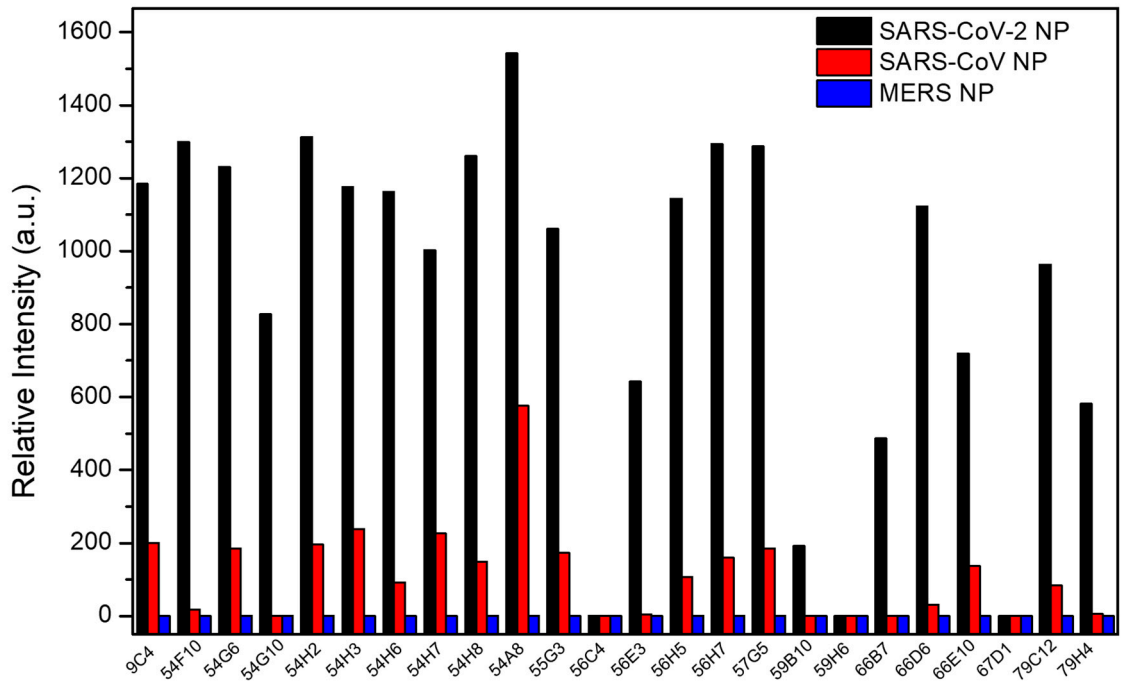



**Figure S3. Bar graph showing secondary screening results using indirect LFIA.** Three different NPs from SARS-CoV-2, SARS-CoV, and MERS-CoV were pre-immobilized onto a nitrocellulose membrane. The ability of the antibody to bind antigen was evaluated by flowing culture solution from a hybridoma containing a specific antibody to the previously immobilized antigen.

**Figure S4**

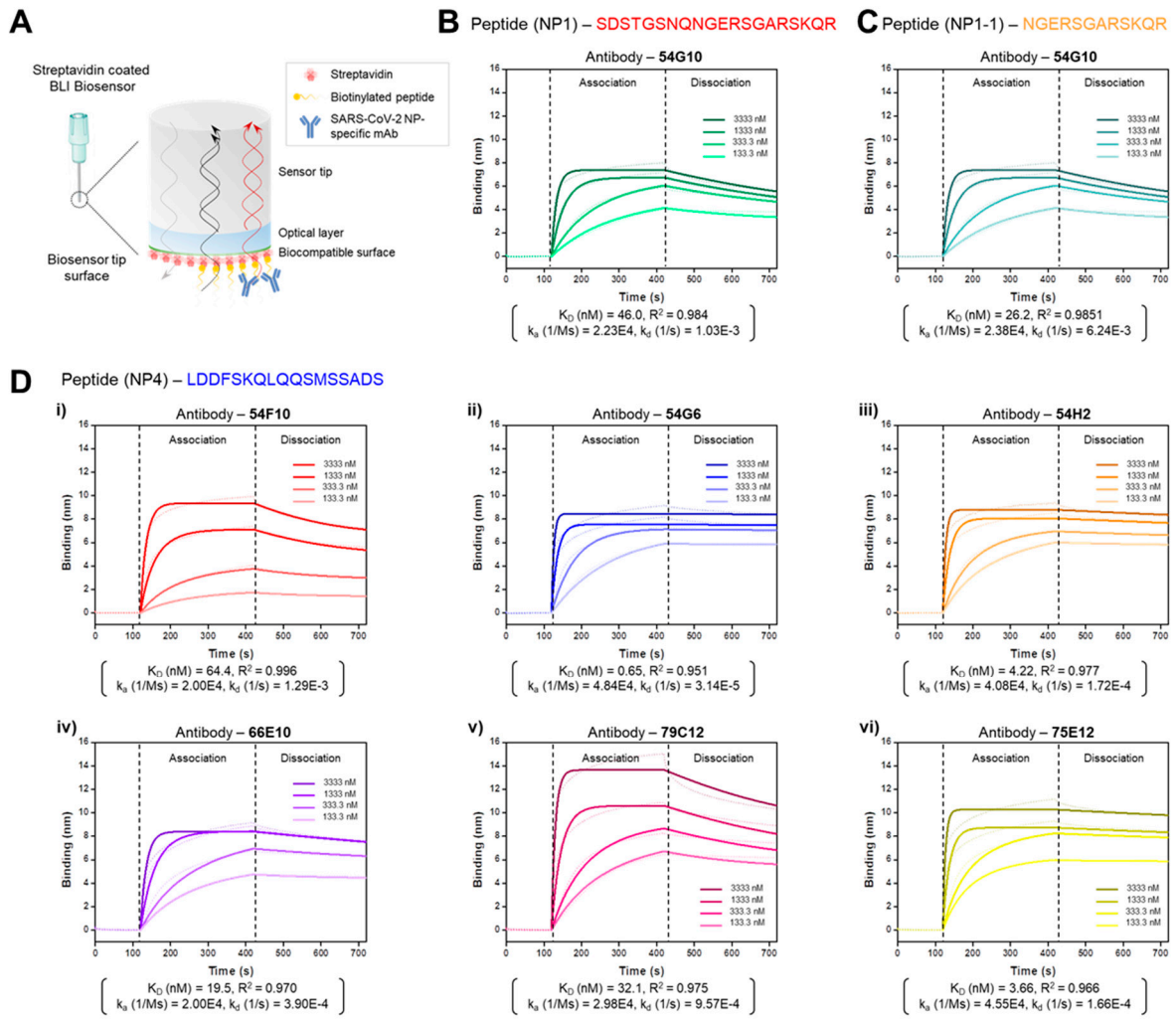



**Figure S4. Biolayer interferometry (BLI) of monoclonal antibodies against antigenic peptides.** A) Schematic illustration of the principle of BLI measurement based on antibody binding. B–D) Association and dissociation curves resulting from binding events between monoclonal antibodies and antigenic peptides. Real-time binding sensorgrams are represented as dotted lines, and their fitting curves are represented as solid lines. Binding constants were calculated from the fitting curves based on a 1:1 binding model.

## Figure S5

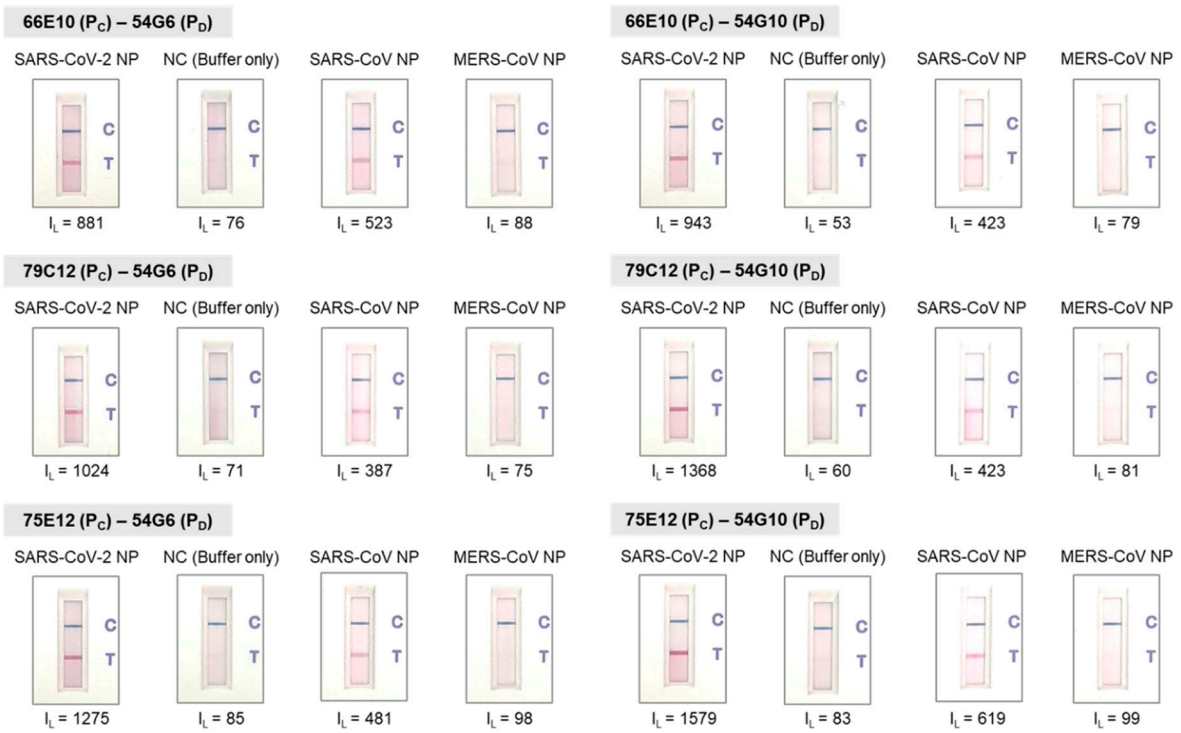



**Figure S5. Brightness and saturation adjusted images of the LFIA results for each of the six pairs.** Six pairs, namely 79C12($P_C$)-54G10($P_D$), 79C12($P_C$)-54G6($P_D$), 75E12($P_C$)-54G10($P_D$), 75E12($P_C$)-54G6($P_D$), 66E10($P_C$)-54G10($P_D$), and 66E10($P_C$)-54G6($P_D$), displayed remarkable detection sensitivity and are selected as sandwich pairs for detecting SARS-CoV-2.

**Figure S6**

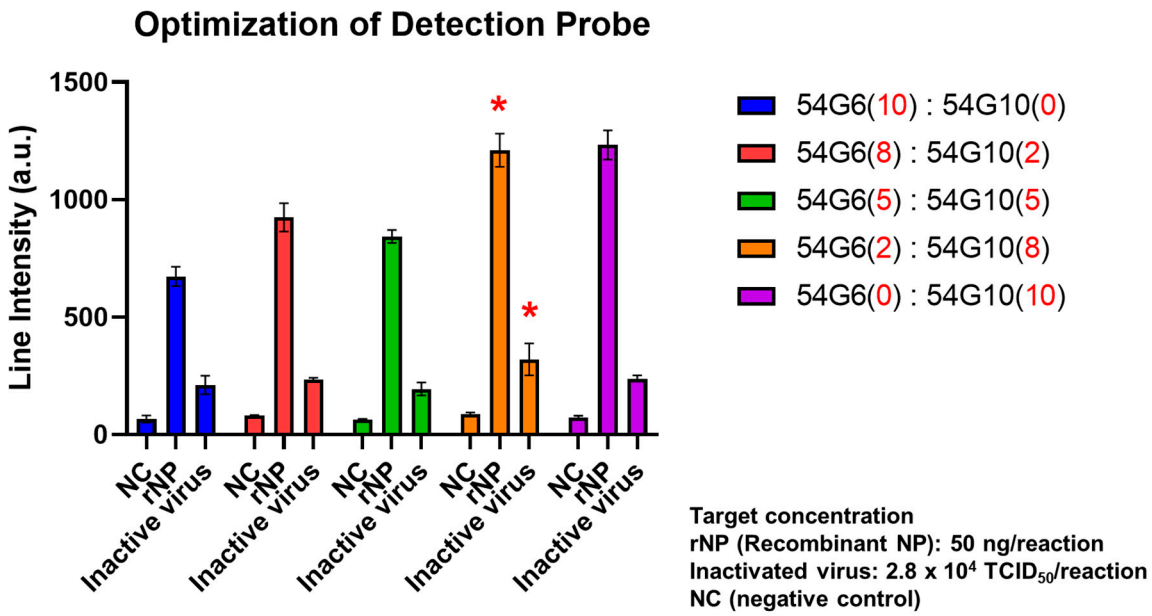



**Figure S6. Optimization of detection probe by adjusting the mixing ratio of 54G6 and 54G10.** Detection probes were optimized by mixing the selected detection probes (54G6 and 54G10) to improve detection sensitivity. Five different mixing ratios were assessed using 50 ng of recombinant SARS-CoV-2 antigen and 2.8 × 104 $TCID_{50}$ of inactivated viral samples. A 2:8 (v/v) ratio was identified as the optimal mixing ratio for detection probes.

**Figure S7**

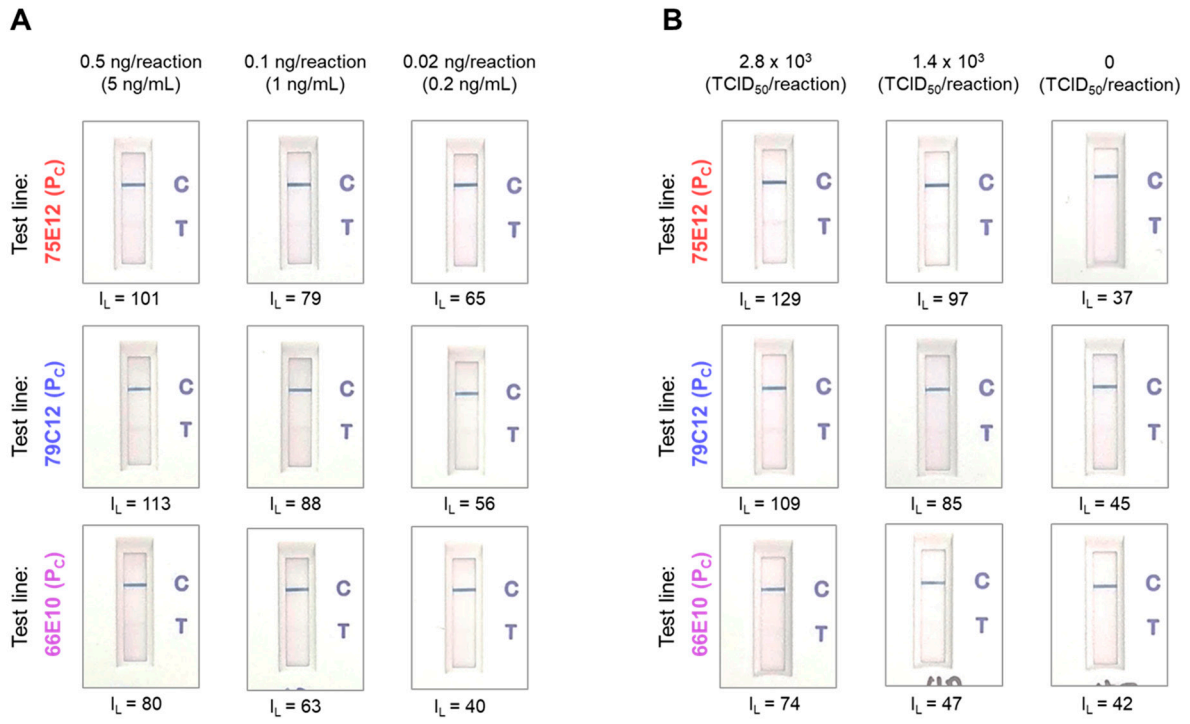



**Figure S7. Brightness and saturation adjusted images of the LFIA results in the low concentration range for the sensitivity analysis.** Three pairs of LFIAs, <Pair 1> 75E12 ($P_C$) – 54G6/54G10 ($P_D$), <Pair 2> 79C12 ($P_C$) – 54G6/54G10 ($P_D$), and <Pair 3> 66E10 ($P_C$) – 54G6/54G10 ($P_D$), are tested using serially diluted samples (concentration ranges – recombinant NP antigen: 0.5 ng to 0.02 ng antigen, viral sample: 5.6 x $10^3$ $TCID_{50}$ to 1.4 x $10^3$ $TCID_{50}$)

## Figure S8

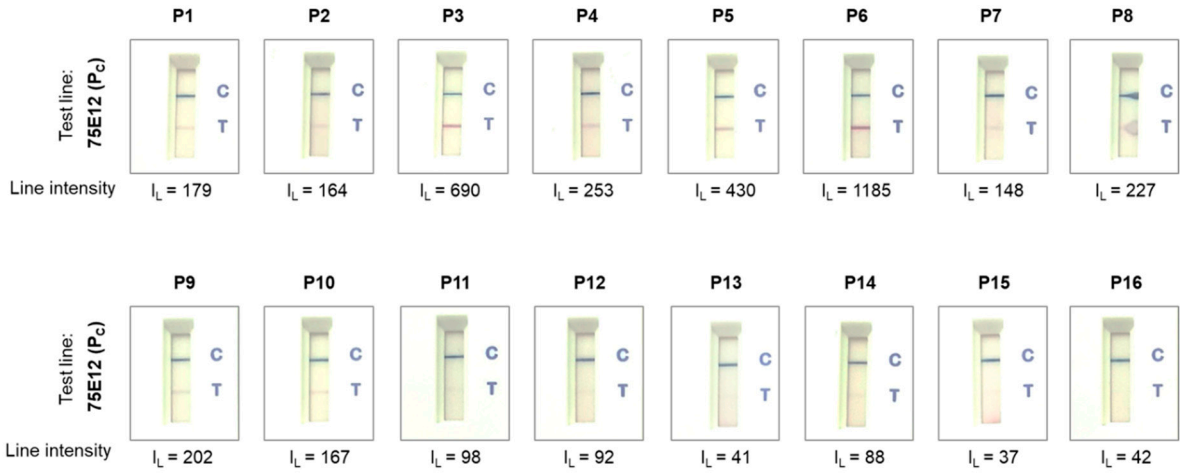



**Figure S8. Brightness and saturation adjusted images of the LFIA results Detection sensitivity results of pair 1-based LFIA with clinical specimens.** Nasopharyngeal swabs from COVID-19 patients (n=16) are applied to the LIFA device. After 15 min of sample loading, the results of COVID-19 infection are confirmed with the naked eye, and the intensities of the test lines are further analyzed with a portable analyzer ($I_L$: line intensity).

## Figure S9

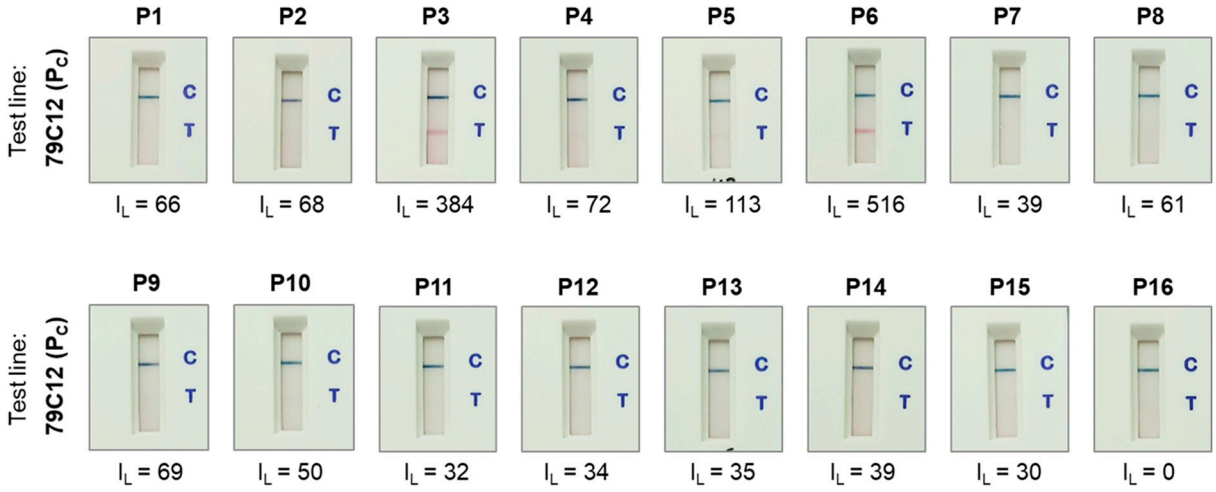



**Figure S9. Detection sensitivity of the Pair 2-based LFIA with clinical specimens.** Sixteen clinical specimens from COVID-19 patients are tested. The Pair 2-based LFIA detected 8/16 patient specimens but failed to detect specimens from patient No. 7, 10, 11, 12, 13, 14, 15, and 16.

## Figure S10

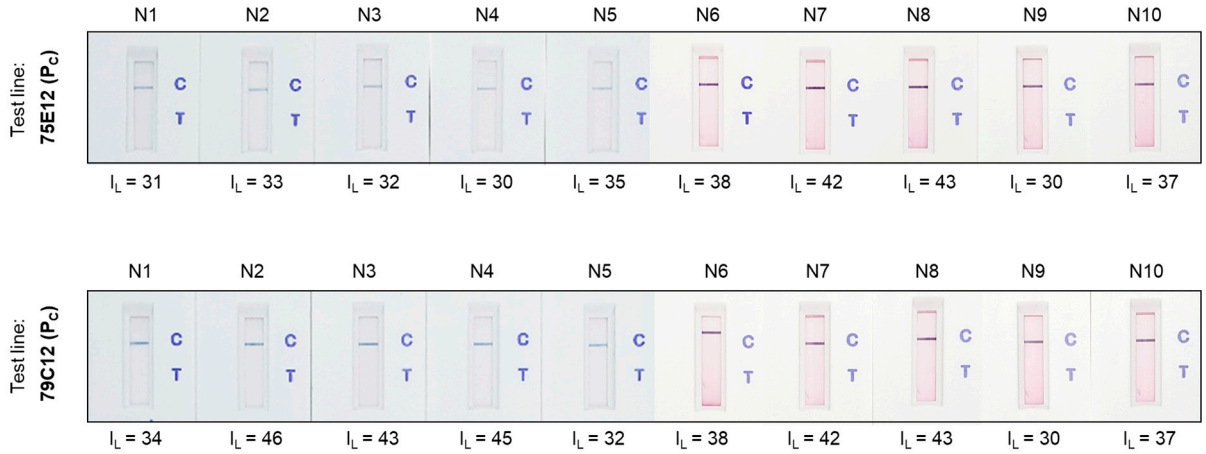



**Figure S10. Pair 1- and Pair 2-based LFIA results using negative samples from healthy donors (n = 10).** There were no false-positive signals for specimens from healthy donors for both Pair 1- and Pair 2-based LFIA.

## Figure S11

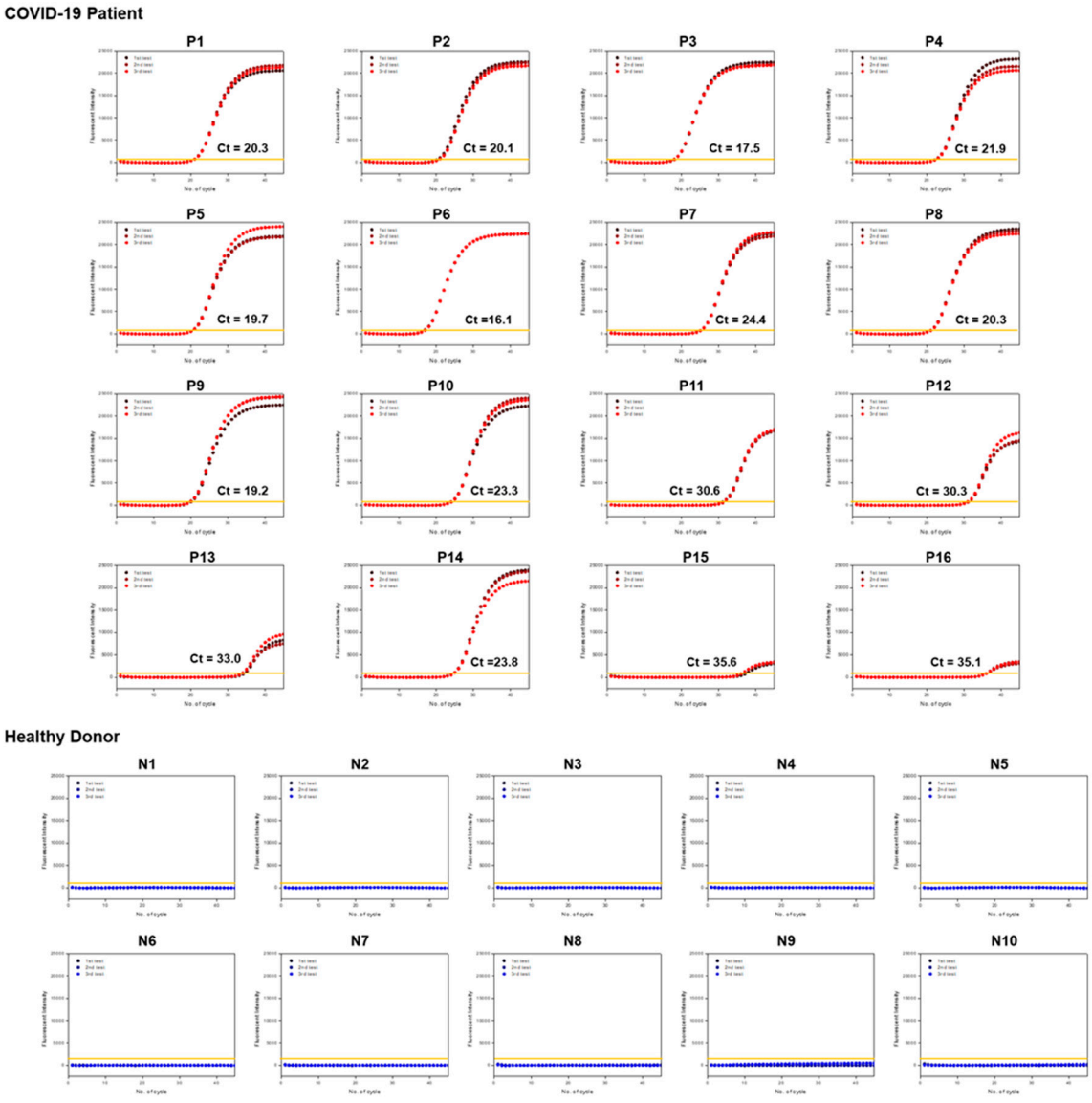



**Figure S11. Results of RT-qPCR analysis with nasopharyngeal swabs from COVID-19 patients (n = 16) and healthy donors (n = 10).** RT-qPCR was performed with specific primer-probe sets to amplify a specific gene (N-gene) of SARS-CoV-2.

**Figure S12**

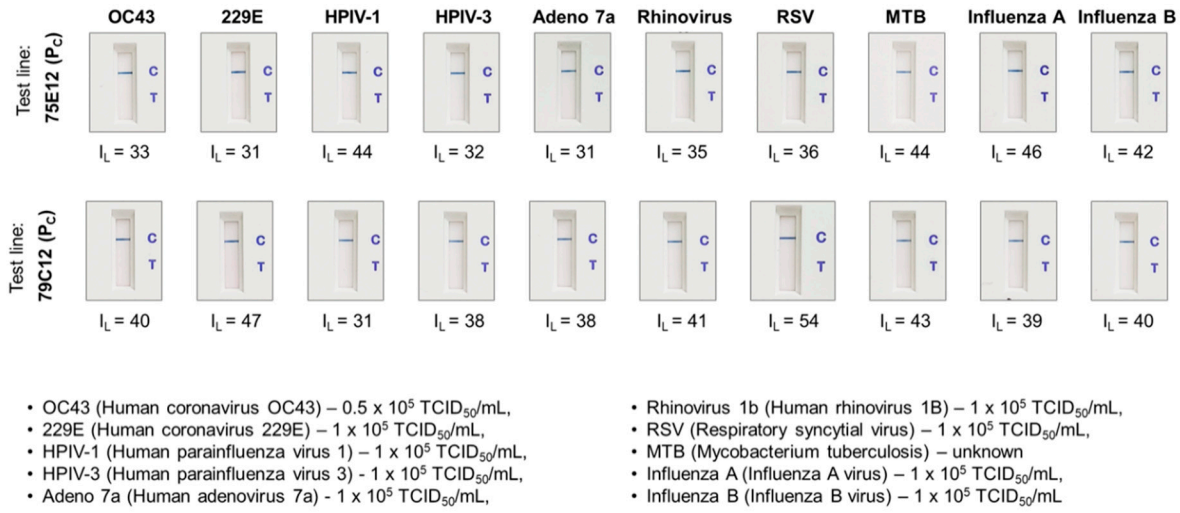



**Figure S12. Analysis of the specificity of Pair 1- and Pair 2-based LFIA.** Representative images of the LFIA specificity test results. Two human coronaviruses (OC43 and 229E) and other respiratory pathogens were tested, including human parainfluenza virus 1 (HPIV-1), human parainfluenza virus 3 (HPIV-3), human adenovirus 7a (Adeno 7a), human rhinovirus 1B (Rhinovirus 1b), human respiratory syncytial virus (RSV), and *Mycobacterium tuberculosis* (MTB). The concentration of the control virus sample was $10^6$ $TCID_{50}$/reaction ($5 \times 10^5$ $TCID_{50}$/reaction for OC43).

**Table S1. Detailed information for COVID-19 patients (n = 16) and healthy donors (n = 10)**

| | Sample ID | Age | Gender | Matrix | Date of hospital admission |
|---|---|---|---|---|---|
| COVID-19 Patient | P1 | 54 | Male | Nasopharyngeal swab | 2020. 12. 08 |
| | P2 | 59 | Female | Nasopharyngeal swab | 2020. 12. 18 |
| | P3 | 33 | Female | Nasopharyngeal swab | 2020. 12. 19 |
| | P4 | 67 | Male | Nasopharyngeal swab | 2020. 12. 24 |
| | P5 | 61 | Female | Nasopharyngeal swab | 2020. 12. 24 |
| | P6 | 44 | Female | Nasopharyngeal swab | 2021. 02. 13 |
| | P7 | 83 | Male | Nasopharyngeal swab | 2021. 02. 16 |
| | P8 | 78 | Female | Nasopharyngeal swab | 2021. 02. 16 |
| | P9 | 35 | Female | Nasopharyngeal swab | 2021. 02. 26 |
| | P10 | 30 | Female | Nasopharyngeal swab | 2021. 02. 28 |
| | P11 | 65 | Female | Nasopharyngeal swab | 2021. 03. 02 |
| | P12 | 23 | Female | Nasopharyngeal swab | 2021. 02. 28 |
| | P13 | 22 | Female | Nasopharyngeal swab | 2021. 02. 26 |
| | P14 | 32 | Female | Nasopharyngeal swab | 2021. 02. 26 |
| | P15 | 68 | Female | Nasopharyngeal swab | 2021. 01. 06 |
| | P16 | 51 | Male | Nasopharyngeal swab | 2021. 01. 12 |
| Healthy controls | N1 | 59 | Female | Nasopharyngeal swab | - |
| | N2 | 47 | Male | Nasopharyngeal swab | - |
| | N3 | 63 | Female | Nasopharyngeal swab | - |
| | N4 | 29 | Male | Nasopharyngeal swab | - |
| | N5 | 41 | Male | Nasopharyngeal swab | - |
| | N6 | 66 | Female | Nasopharyngeal swab | - |
| | N7 | 66 | Male | Nasopharyngeal swab | - |
| | N8 | 50 | Male | Nasopharyngeal swab | - |
| | N9 | 34 | Male | Nasopharyngeal swab | - |
| | N10 | 29 | Male | Nasopharyngeal swab | - |